

In-situ U-value measurements of wood frame roofs: analysis of deviations between measured and design performance

A. Janssens, Building Physics Group, Faculty of Engineering and Architecture, Ghent University, Belgium
IEA-Annex 58, Working Meeting München, april 8-10, 2013.

Contribution to subtask 2: Optimising full scale dynamic testing

ABSTRACT

The hygrothermal performance of various lightweight sloped roof designs was monitored in the KULeuven VLIET testbuilding for 2 years (Janssens et al. 1998). One of the aims of the investigation was to evaluate whether the design U-value of $0.18 \text{ W/m}^2\text{K}$ was effectively met in practice. For this reason 3 heatflux transducers were installed at the inside surface of each component together with a number of thermocouples at the surfaces of the composing material layers. The U-value was derived from the measurements by averaging the collected data on a daily basis. The observed deviations between the measured and design U-values are analysed and explained by quantifying the inconsistencies between the assumptions for the calculation of the design thermal performance and the conditions of the in-situ measurement. The following causes of deviations are analysed in detail, and related to the position of the heat flux transducer on the test components:

- heat transport affected by wind-washing in the roofs
- 2-dimensional heat flow through framing elements in the roofs

Test Roofs

In order to evaluate the effective performance of different well-insulated roof designs, a long-term field testing programme was carried out on four types of tiled wood frame roofs. It was the objective to investigate whether a good thermal quality ($U = 0.2 \text{ W/(m}^2\text{K)}$) is achievable with current residential construction systems and practices. The measured thermal performances of the roof components are compared to the design values, and related to the wind speeds and directions registered near the test building.

The field measurements were performed in a test building at K.U.Leuven (near Brussels), specially developed to evaluate energy-efficient and durable building envelope designs (Roels 2011). The facility allows the simultaneous testing of twenty wall systems, four flat roofs and six duo-pitched roof systems exposed to the cool and humid West-European climate. The building is rectangular in shape, with the measuring bays located in the longitudinal facades, directed to the northeast and the southwest. In Western Europe, southwest is the direction of prevailing winds, wind-driven rains and solar irradiation, while north-east hardly receives any sun and rain. In the test building different indoor climates may be imposed by means of an air-conditioning system with local steam humidifiers and a temperature and humidity control. Air pressure differences between the inside and outside are managed through ventilation grids in the entrance doors and fans in the HVAC system.

The building has its own weather station located above the ridge of the sloped roofs module at 10 m above ground level. It registers the outside climate parameters on a one minute basis (temperature, humidity, wind speed and direction, global solar irradiation, horizontal rainfall). The inside temperature and relative humidity are stored as ten minute means.

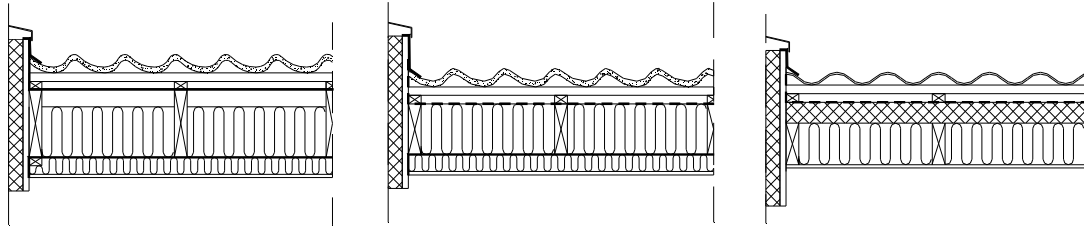


Figure 1: Lay-out of the vented roof type (left), the compact roof type (middle) and the retrofit roof (right). Of the vented and compact roof type a variant with and without a polyethylene (PE) air barrier in between the cavity and interior insulation layer was tested.

Table 2: Test roofs classification

TEST ROOF	VENTILATION	PE-AIR BARRIER	UNDERLAY
VENTED	cavity 50 mm	NO	bituminous felt overlaps every 0.9m
VENTED with PE	cavity 50 mm	YES	
COMPACT	NO	NO	spunbonded PP overlaps every 1.4m
COMPACT with PE	NO	YES	
RETROFIT	NO	NO	XPS 60 mm + spunbonded PP

The study related to five tiled wood frame roof designs, typical of residential roof construction in Western Europe. The test roofs were 1.8m wide and 5.1m long per pitch. Roof slope was 45°. Figure 1 shows the roof designs tested. The first four test roofs contained the following layers (from the outside): (1) concrete tiles on laths and battens, (2) underlay film, (3) 14 cm fibre glass insulation in between rafters, (4) 5 cm fibre glass interior insulation in between horizontal furring and (5) painted gypsum board. As in practice, the overlaps in the underlays were left unsealed. These four test roofs differed in the material of the underlay, in the presence of a vented cavity below the underlay and in the presence of a polyethylene air barrier. Table 1 gives a classification of the different roof systems.

Two of these roofs were so-called vented roofs, containing a vented air cavity in between the thermal insulation and the underlay. The ridge and eaves of the vented roofs were detailed with ventilation openings in order to enhance the flow of outside air into the cavity below the underlay. The underlay material in this type of roof consisted of a bituminous felt, with horizontal overlaps every 90 cm. The two other test roofs were of the so-called compact type, meaning that the thermal insulation filled the structural cavity completely. The underlay material was spunbonded polypropylene, which combines a sufficient air and water tightness with a high vapour permeance. The underlay of the compact roofs had horizontal overlaps every 1.40 m. Both the vented as the compact roof types had a test roof equipped with a polyethylene (PE) air barrier in between the cavity and the interior insulation layer, and another test roof without this air barrier. The PE air barrier was stapled at the rafters. In the gypsum board and the PE air barrier all joints and intersections were sealed. This way all test roofs were intended to achieve a sufficiently low air permeance to minimize air leakage through the systems.

The fifth roof represented a retrofit solution for existing woodframe roofs that need thermal upgrading. This section contained the following layers (from the outside): (1) corrugated fibre cement plates on laths and battens, (2) PP underlay film, (3) 6 cm extruded polystyrene board mounted on top of the rafters, (4) 12 cm fibre glass insulation in between rafters and (5) painted gypsum board (Figure 1).

The measuring equipment consisted of heat flux transducers applied at the inside of the internal linings and thermocouples at all material interfaces and at 3 heights. The heat flux sensors were located central between the vertical and horizontal structural elements, according to the instructions of ASTM C1155 and ISO 9869. In the roofs with PE air barrier and in the retrofit solution, the heat flux was measured in the middle of each pitch only. In the pitches without PE air barrier, the heat flux was measured additionally at 1 m from the eaves and ridge. Measuring results were stored as 10'-means. All heat flux transducers were recalibrated at the end of the test period.

Table 2: Measured material properties

LAYER	d (mm)	ρ (kg/m ³)	λ (W/m/K)	K_a (m/s/Pa)
spunbonded PE	0.5			$160 \cdot 10^{-6}$
bituminous felt	1.7			$1 \cdot 10^{-6}$
Extruded polystyrene	60	37	$0.0246 + 0.9 \cdot 10^{-4} \cdot \theta$	
Cavity insulation	140	18	$0.0320 + 2.2 \cdot 10^{-4} \cdot \theta$	$\pm 1000 \cdot 10^{-6}$
PE air barrier	0.2			$< 1 \cdot 10^{-6}$
interior insulation	50	13	$0.0375 + 2.3 \cdot 10^{-4} \cdot \theta$	$\pm 5000 \cdot 10^{-6}$
Painted gypsum board	12.5	660	0.13	$< 1 \cdot 10^{-6}$

The measured heat and air transfer properties of all materials are listed in Table 2. The design thermal properties of the test roofs are calculated on the basis of the measured thermal conductivities. The design clear roof U-value of the vented and compact roof types is equal to 0.18 W/m²/K. With thermal bridging through the wooden roof structure (rafters and furring) taken into account, the mean U-value amounts to 0.21 W/m²/K. For the retrofit solution, the design clear U-value is 0.17 W/m²/K, while the mean U-value including heat transfer through rafters is 0.18 W/m²/K.

Measured thermal performance

The in-situ mean thermal resistance R of the roofs was determined from the measured mean heat flux q and the measured mean temperatures at the interior surface θ_{si} and the underlay θ_{ul} , according to ASTM C1155 and ISO 9869. In order to separate the effect of wind-driven convection from other factors influencing the effective thermal performance, the measuring results were expressed in the form of daily-averaged Nusselt numbers, defined by the ratio between a reference thermal resistance measured during windless days and the thermal resistance measured during 24h-periods. A day was called windless when the mean wind velocity was below 0.5 m/s. The Nusselt numbers thus defined the relative increase of heat losses through the roofs as a result of wind-driven convection:

$$Nu = \frac{R_{ref}}{R} \quad (1)$$

$$\text{with: } R = \frac{\sum_{24h} (\theta_{si} - \theta_{ul})}{\sum_{24h} (q_{si})} \quad (2)$$

$$R_{ref} = n \cdot \left[\sum_{i=1}^n \frac{1}{R_i|_{v \leq 0.5 \text{ m/s}}} \right]^{-1} \quad (3)$$

Finally the reference clear roof thermal transmittance was calculated as:

$$U_{ref} = \left[R_{ref} + \frac{1}{h_i} + \frac{1}{h_e} \right]^{-1} \quad (4)$$

Here h_i is the standardized surface film coefficient at the inside surface, and h_e is the equivalent surface film coefficient at the outer underlay surface, taking into account the thermal shielding of the tiles. Both were set equal to 8 W/(m²/K) according to standard EN ISO 6946. The maximum measuring error in the derived U-value is estimated at 0.01 W/(m²/K).

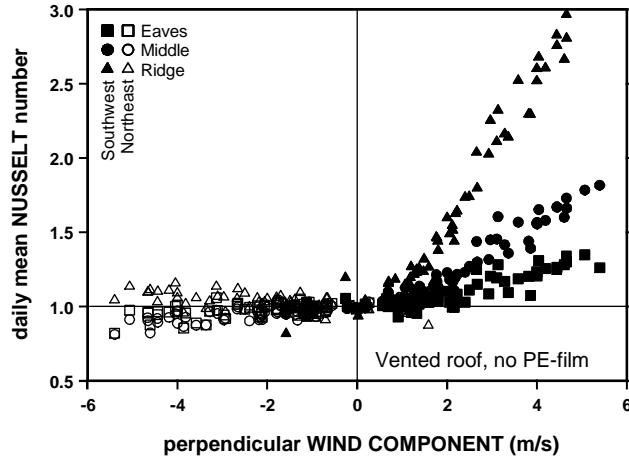


Figure 2: Measured Nusselt numbers as a function of the perpendicular wind speed component in the vented roof type without PE air barrier (daily mean data).

This analysis was applied to measuring data during the winter months (December 19-March 8). During this period the average outside temperature was 7.6°C, the inside temperature was 22.7°C, and the average local wind speed was 2.4 m/s. For comparison the clear roof thermal transmittance U_{avg} was also derived as an average over the entire measurement period, without separating the effect of wind-driven convection. Therefore this transmittance is called the 'apparent' U-value, quantifying the mean relation between temperature difference and heat flux (be it by conduction or convection).

Figure 2 shows a typical relationship between the measured daily mean Nusselt numbers and the measured daily mean wind speed components perpendicular to the roof surfaces of the test roofs. The perpendicular wind speed component is defined by:

$$v_{\perp} = v \cdot \cos(\alpha_w - \alpha_n) \quad (6)$$

where v is the wind speed (m/s), α_w is the wind direction (degrees from north) and α_n is the direction of the normal to the roof surface (45° for the northeast and 225° for the southwest oriented pitch). The perpendicular wind speed component is positive when the roof pitch is windward and negative when it is leeward. As the wind was blowing from the southwest most of the time the perpendicular wind speed component was almost always positive along the southwest pitch and negative along the northeast pitch.

Table 3 and Figure 3 show the results of the thermal analysis of the measuring data: the apparent U-value U_{avg} averaged over the entire measurement period, the reference U-value U_{ref} derived from the heat flux data in the test roofs during windless days, and the Nusselt number at a southwest wind of 4 m/s, corresponding to the normal meteorological wind speed in Belgium. The Nusselt number is defined from a cubic function fitted to the daily mean measuring data using the linear least squares method.

In general the apparent measured U-values U_{avg} meet the design targets in the retrofit roof and in the northeast-oriented vented and compact roofs. In the southwest-oriented vented and compact roofs however measured values are systematically higher than the design values, locally up to 0.10 W/m²K or 55%. The differences between measured and design values are reduced when effects of wind-driven convection are separated in the compact and vented roofs. The measured clear roof thermal transmittances U_{ref} agree reasonably well with the design value of 0.18 W/(m²K), up to differences of 0.02 W/m²K or 10%.

As the table and figure show, the established effects of wind driven convection on the apparent heat loss depend on the roof design, the orientation of the pitch and the distance from the ridge. The thermal performance of the roofs with additional PE air barrier is not strongly affected by the wind, with Nusselt numbers at a wind speed of 4 m/s in between 0.92 and 1.06. On the other hand, the thermal performance of the test roofs without PE air

barrier is strongly related to the wind. In the windward pitch the relative heat loss considerably increases with wind speed and from the eaves to the ridge. This effect is the most important in the vented roof, with local Nusselt numbers above 2.5 at wind speeds higher than 4 m/s. The Nusselt numbers measured in the compact roof are generally smaller than in the vented roof, but still show an important increase of the heat loss at the windward pitch. At the leeward side on the other hand, the compact roof without PE-air barrier shows a significant heat loss reduction (Nusselt numbers smaller than 1).

Globally the measuring results suggest that wind tightness of the underlay should be a prime performance requirement in sloped insulated roofs, and consequently that the continuity of the underlay is a point of attention. Janssens and Hens (2007) give a more detailed explanation of the thermal effects of wind driven convection using tracer gas tests to show the pattern of wind driven air flow in the roofs.

Table 4: Measured thermal performance in the test roofs

TEST ROOF	NORTHEAST PITCH			SOUTHWEST PITCH				
	U_{avg} W/m ² K 19/12-08/03	U_{ref}^* W/m ² K	Nu $v_{SW} = 4.0$ m/s	U_{avg} W/m ² K 19/12-08/03	U_{ref}^* W/m ² K	Nu $v_{SW} = 4.0$ m/s		
VENTED ($U_{design} = 0.18$ W/m ² K)	without PE-film	bottom	0.17	0.18	0.95	0.19	0.18	1.22
		middle	0.19	0.20	0.92	0.22	0.19	1.55
	with PE-film	top	0.18	0.18	1.06	0.28	0.19	2.52
		middle	0.18	0.18	0.99	0.21	0.21	1.06
COMPACT ($U_{design} = 0.18$ W/m ² K)	without PE-film	bottom				0.21	0.19	1.28
		middle	0.17	0.18	0.73	0.22	0.20	1.37
		top	0.16	0.17	0.75	0.18	0.16	1.59
	with PE-film	middle	0.17	0.17	1.02	0.19	0.19	0.92
RETROFIT ($U_{design} = 0.17$ W/m ² K)	middle	0.16			0.15			

* from data on three days with daily mean wind speed < 0.5 m/s

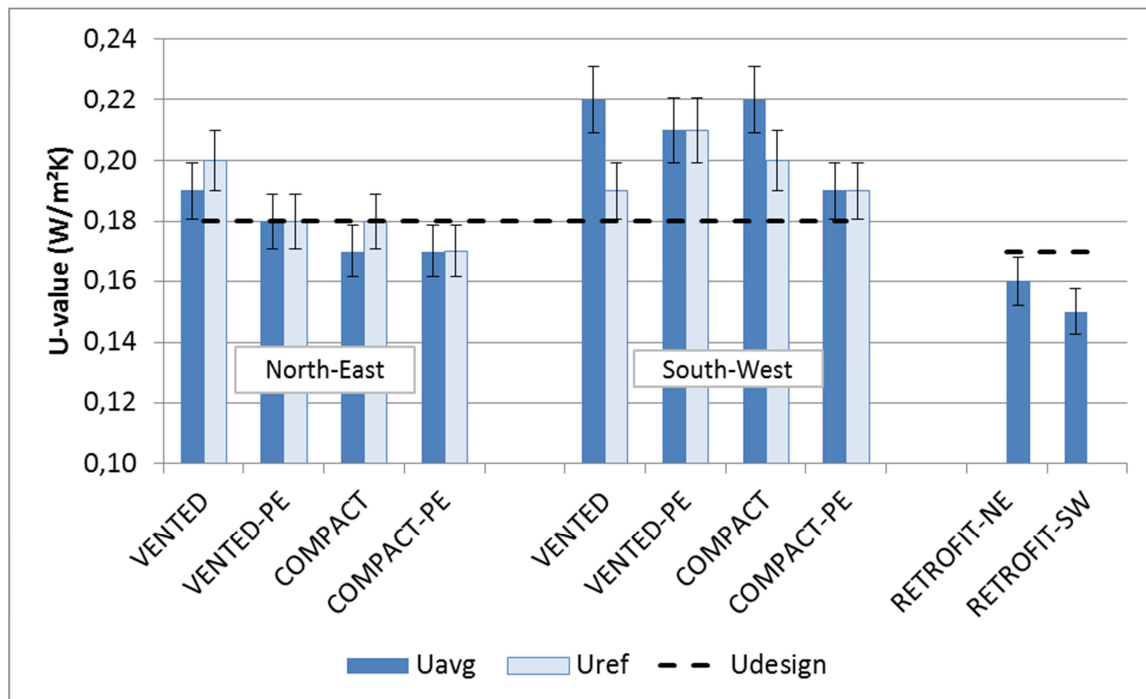


Figure 3: comparison between the test roofs design U-values, the apparent U-values U_{avg} averaged over the entire measurement period, and the reference U-values U_{ref} derived during windless days (results of heat flux sensors in middle position with $\pm 5\%$ measuring uncertainty).

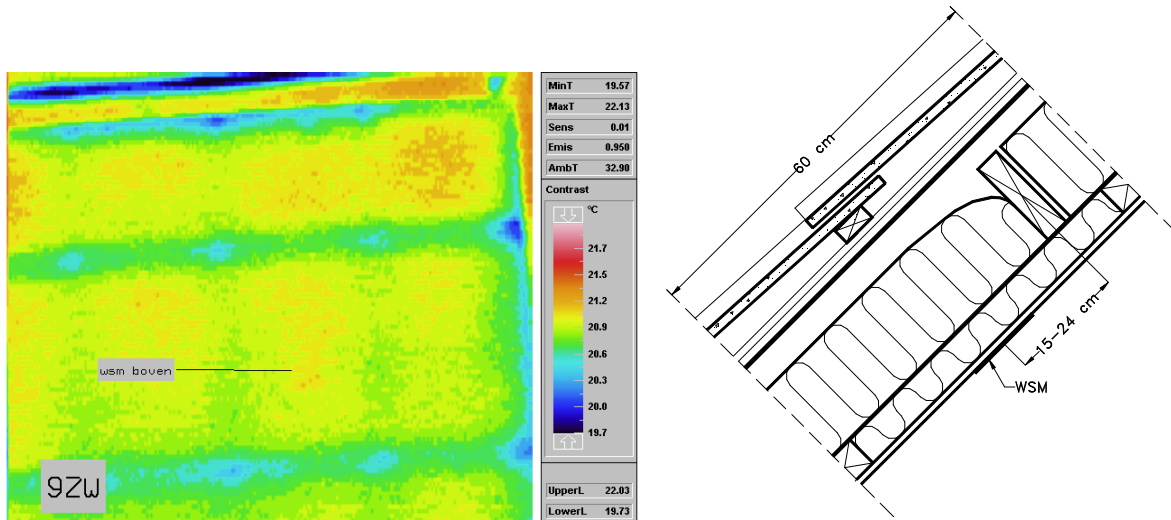


Figure 4: Interior surface thermography (left, compact roof) and vertical section (right, vented roof), showing the position of the heat flux transducers relative to the position of framing elements (left: position near ridge, right: middle position)

Influence of 2-dimensional heat flow through framing elements

Although the differences between measured and design values are reduced when effects of wind-driven convection are separated in the compact and vented roofs (Figure 3), there are still deviations up to 0.03 W/m²K (15%) between both values. Furthermore it is remarkable that if the measured values in the vented and compact roofs deviate from the design values, the measured U-values are typically higher than the design values, while for the retrofit roofs the measured values are systematically lower (up to 0.02 W/m²K).

These differences may be explained by the inconsistencies between the assumptions for the calculation of the design thermal performance (1D-heat conduction through the material layers) and the conditions of the in-situ measurement. Although the heat flux sensors were located central between the vertical and horizontal structural elements as much as possible (Fig. 4), the influence of 2-dimensional heat flow on the heat flux transducer readings may not be eliminated. Also minor excentricities between the position of heat flux transducers and the symmetry planes between framing elements are possible in the test set-up. The influence of framing elements is analysed in this section by means of 2D heat transfer simulations.

The influence of three framing elements have been analysed, both in the compact and vented roofs, and in the retrofit roof:

- 38 mm wide vertical rafters, center to center distance 440 mm
- 38 mm wide horizontal element (present in the middle of each pitch, see figure 4b)
- 70 mm wide horizontal furrings, center to center distance 600 mm (not present in retrofit roof).

As an input for the calculations, we use the measured temperature-dependent thermal conductivities for the insulating materials and a thermal conductivity of 0.14 W/(mK) for the wooden framing elements. The 2D heat transfer programme calculates the heat fluxes at the inner surface and the temperatures at all the material interfaces as a function of the distance x from the axis of the framing element. This way it is simulated which thermal resistance would follow from the measurement if the heat flux transducer and the thermocouple would be attached at the position x on the inner surface. Assuming the side of the heat flux transducer is 0.1 m, the apparent thermal resistance at a distance x from the framing element follows from:

$$R_s(x) = \frac{\theta_{si}(x) - \min(\theta_{OD})}{x + 0.05 + \int_{x-0.05}^x q(x) dx / 0.1} \quad (7)$$

Figures 5-7 show the relative deviation between apparent thermal resistances following from the 2D simulations, and the one-dimensional design thermal resistance as a function of the distance from the framing element. The geometrical input for the simulations is also shown. A positive value for the relative deviation means that the measured thermal resistance is higher than the design value. The influence of the vertical rafters results in systematic deviations between measured and design values. In the retrofit roofs, the presence of rafters at a distance of 22 cm on both sides of the heat flow meter results in a systematic increase of the measured thermal resistance of 3% compared to the design value (Figure 5). In the vented and compact roofs, the presence of the rafters results in a reduction of the measured thermal resistance of 3% compared to the design value (Figure 6). An excentric position of the heat flux transducer results in larger deviations. These findings are consistent with the results of the measurements (Figure 3). The influence of the horizontal furrings in the vented and compact roofs appears to be small with respect to the influence of the rafters (Figure 7).

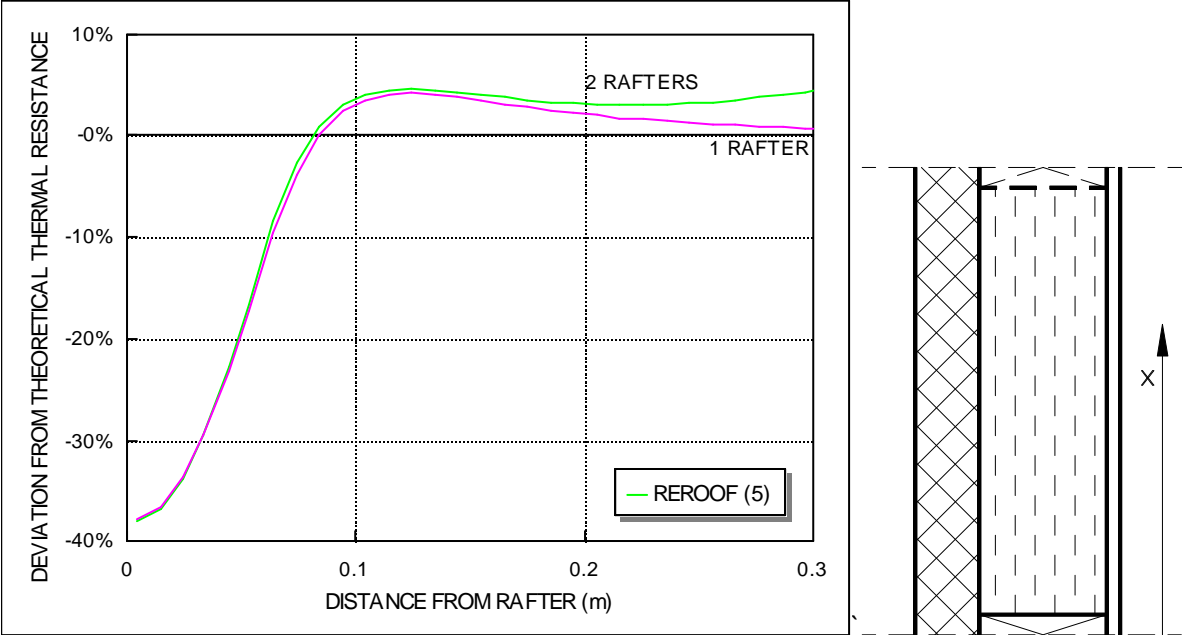


Figure 5: Simulated influence of rafters in retrofit roof

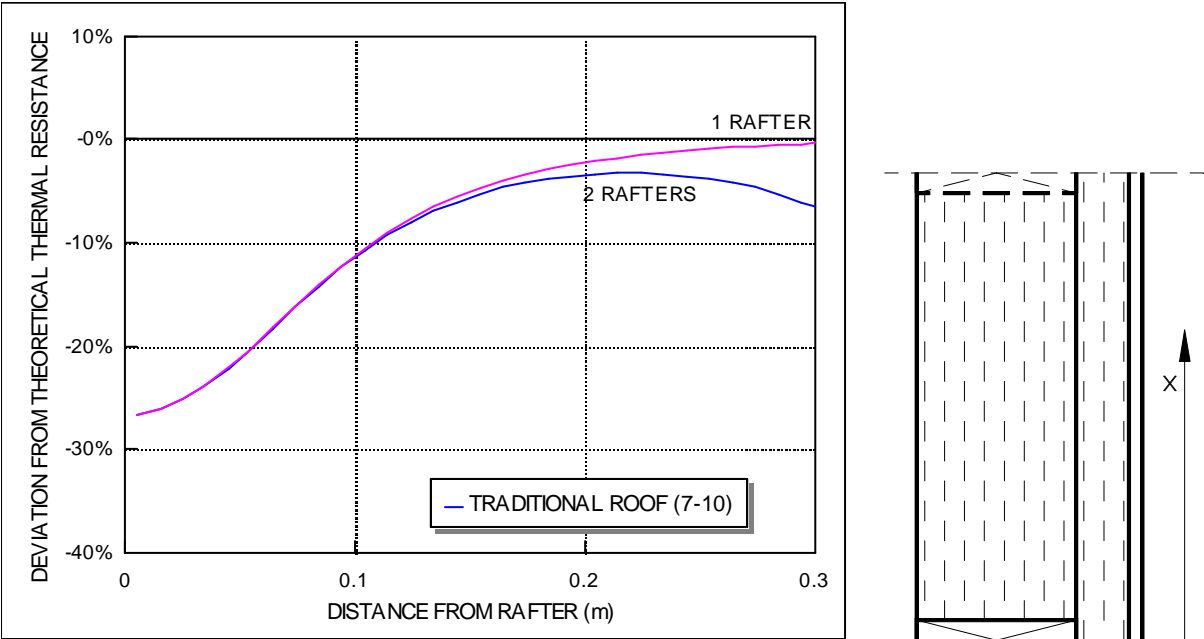


Figure 6: Simulated influence of rafters in vented and compact roofs

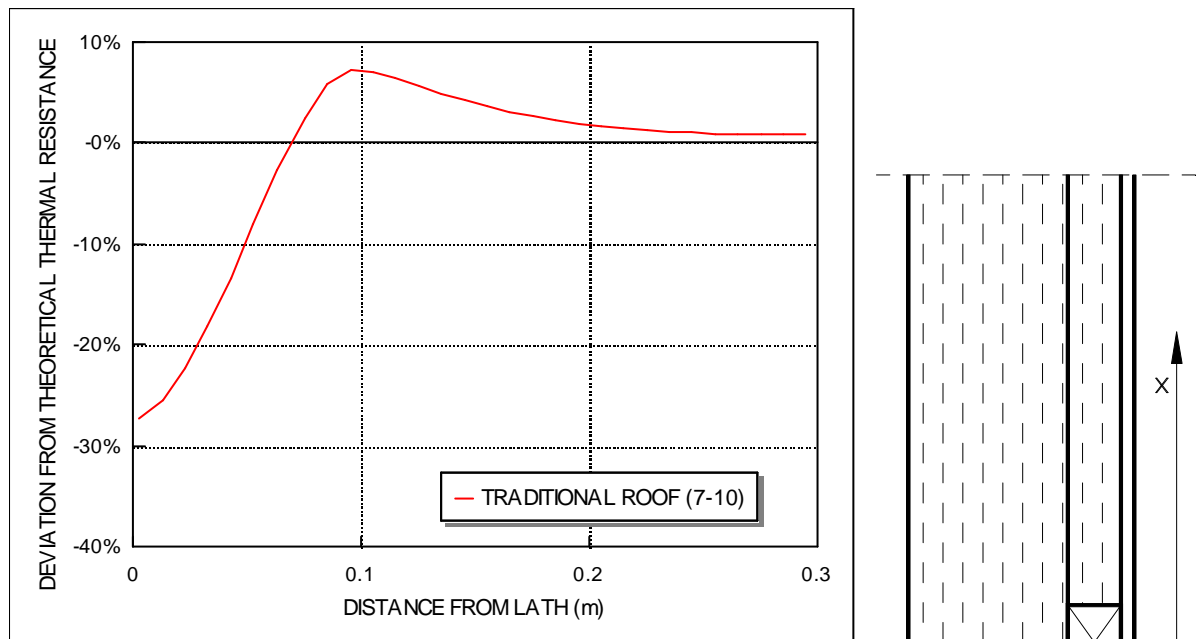


Figure 7: Simulated influence of horizontal furrings in vented and compact roofs

The heat flux transducers positioned in the middle of a pitch were also influenced by the presence of a horizontal element (Figure 4b). When constructing the roof, these elements had been installed by the carpenters as a traditional crossbar. However, since these elements had not been drawn on the design plans, their position was not exactly known, and was not taken into account when the heat flux transducers had been installed. After inspection it appeared that the distance between the horizontal elements and the middle heat flux transducers was in between 12 and 24 cm. The observed variation in distance in the vented and compact roofs results in a reduction of the measured thermal resistances between 1% and 8% compared to the 1D design value, on top of the 4% reduction caused by the presence of the vertical rafters (Figure 6). These calculations only take the influence of the crossbar into account, and not the possible defects in the thermal insulation near the connection with the crossbar. It goes without saying that if the insulation in the vicinity of the crossbar is compressed, the deviation of the measured thermal resistance as a result of the presence of the crossbar is more negative than what was calculated.

Conclusions

This paper presented measuring results of the thermal performance of duo-pitched tiled wood frame roof designs, with a design thermal transmittance U of $0.18 \text{ W/m}^2\text{K}$. The measurements showed that the thermal performance may be affected considerably by wind driven convection. The magnitude of the wind effect depended on the orientation of the pitch relative to the wind direction, the location of the air barrier relative to the insulation layer and the presence of a ventilation cavity above the insulation layer. The compact roof type was less vulnerable to the effects of wind washing than the vented roof type.

In order to separate the effect of wind-driven convection from other factors influencing the effective thermal performance, the measuring results were expressed in the form of daily-averaged Nusselt numbers, defined by the ratio between a reference thermal resistance measured during windless days and the thermal resistance measured during 24h-periods. The remaining deviations found between the measured reference and the design thermal performance could be explained by considering the 2D heat transfer in the various wood frame elements in the roofs. Even though the heat flux sensors were located central between the vertical and horizontal framing elements as much as possible, the influence of 2-dimensional heat flow on the heat flux transducer readings could not be neglected. Depending on the eccentricity of sensor positions and the presence of specific wood frame elements deviations could be in between 3 and over 10% compared to the 1D design values.

References

- ASTM C1155. Standard practice for determining thermal resistance of building envelope components from in-situ data. Annual book of ASTM standards. ASTM, PA, 2007.
- INTERNATIONAL STANDARD Thermal insulation – Building elements - In-situ measurement of thermal resistance and thermal transmittance ISO 9869:1994 (E), 2009
- Janssens, A., W. Depraetere, A. Morel and H. Hens. 1998. VLIET test building, third and final yearly report (in Dutch), internal report research contract IWT/VLIET/930235, Laboratory of Building Physics, K.U.Leuven, Belgium.
- Janssens A. and H. Hens. 2007. Effects of wind on the transmission heat loss in duo-pitched insulated roofs: a field study, Energy and Buildings , Vol. 39/9, 1047-1054
- Roels, S. 2011. VLIET testbuilding KULeuven. Full scale test facilities for evaluation of energy and hygrothermal performances (Janssens, A, Roels S, Vandaele, L, ed.). ISBN 978-94-9069-584-2, BFG, UGent, Belgium, 7-14.